AIMS Mathematics, 7(6): 11362–11381.
DOI:10.3934/math.2022634
Received: 21 December 2021
Revised: 16 March 2022
Accepted: 24 March 2022
Published: 12 April 2022

http://www.aimspress.com/journal/Math

Research article

New applications related to hepatitis C model

Nauman Ahmed[1], Ali Raza[2], Ali Akgül[3,*], Zafar Iqbal[1,4], Muhammad Rafiq[5], Muhammad Ozair Ahmad[1] and Fahd Jarad[6,7,8,*]

[1] Department of Mathematics and Statistics, The University of Lahore, Lahore, Pakistan
[2] Department of Mathematics, Govt. Maulana Zafar Ali Khan Graduate College Wazirabad, 52000, Punjab Higher Education Department (PHED), Lahore, 54000, Pakistan
[3] Siirt University, Art and Science Faculty, Department of Mathematics, 56100 Siirt, Turkey
[4] Department of Mathematics, University of Management and Technology, Lahore, Pakistan
[5] Department of Mathematics, Faculty of Science, University of Central Punjab, Lahore, Pakistan
[6] Department of Mathematics, Cankaya University, Etimesgut 06790, Ankara, Turkey
[7] Department of Mathematics, King Abdulaziz University, Jeddah, Saudi Arabia
[8] Department of Medical Research, China Medical University Hospital, China Medical University, Taichung, Taiwan

* **Correspondence:** Email: aliakgul00727@gmail.com, fahd@cankaya.edu.tr; Tel: +905304616538.

Abstract: The main idea of this study is to examine the dynamics of the viral disease, hepatitis C. To this end, the steady states of the hepatitis C virus model are described to investigate the local as well as global stability. It is proved by the standard results that the virus-free equilibrium state is locally asymptotically stable if the value of R_0 is taken less than unity. Similarly, the virus existing state is locally asymptotically stable if R_0 is chosen greater than unity. The Routh-Hurwitz criterion is applied to prove the local stability of the system. Further, the disease-free equilibrium state is globally asymptotically stable if $R_0 < 1$. The viral disease model is studied after reshaping the integer-order hepatitis C model into the fractal-fractional epidemic illustration. The proposed numerical method attains the fixed points of the model. This fact is described by the simulated graphs. In the end, the conclusion of the manuscript is furnished.

Keywords: hepatitis C model; fractional derivatives; stability analysis; numerical simulations
Mathematics Subject Classification: 65P99, 92D25, 92-10

Abbreviations: HAV: Hepatitis A virus; HBV: Hepatitis B virus; HCV: Hepatitis C virus; DAA: Direct-Acting antiviral; US: United States of America; KPK: Khyber Pakhtunkhwa;

SCTZ: Susceptible-Chronically infected-On treatment-Failed treatment; TIV: Uninfected hepatocytes-Productively infected hepatocytes-Virus; TIVA: Target cells-productively infected cells-viral load-ALT concentration; SEI_aI_cTR: Susceptible-Exposed-Acute infection-Chronic infection-Treated-Recovered; RTPE: Plus-strand HCV RNA molecules-Translation complexes, HCV polyprotein molecules-Enzyme NS5B; SIAB: Susceptible-Infectious not in treatment-Infectious with treatment-Infectious individuals who are on treatment with intravenous drug misuse; TIVZWA: Uninfected cells-Infected cells-Free virus numbers-CTL response-Antibody response-ALT levels; DFE: Disease free equilibrium; EE: Endemic equilibrium; G.A.S: Globally Asymptotically Stable

1. Introduction

The liver is an important organ in the human body, it filters the blood, maintains body temperature plays a role in digestion, has a key role in the immune system, and also acts as a store house for food. Inflammation in the liver is called hepatitis. There are different types of hepatitis such as hepatitis A, B, C, D, E. They can also be written as HAV, HBV, HCV., etc. Hepatitis C is caused by a virus, member of the family Flaviviridae. This virus damages the liver and affects its functions. This virus cannot spread through man to man, but only through affected blood, i.e., contaminated blood. Toothbrushes, razors, syringes, and nail clippers are easy sources of its transmission. This virus can survive at least four days outside the body in an open environment. HCV shows a few symptoms, so most people do not aware of it, which makes it to fatal. 80% of HCV patients do not show any symptoms. Some common symptoms are bleeding, fatigue, lack of appetite, yellow coloration of skin especially the eyes, dark yellow color of urine, etc. Its incubation period varies from 2 weeks to 6 months. Hepatitis C virus grows in several stages, some of which are explained as follows. Acute hepatitis C is short time infection and the patient faces this infection for up to several months. Its symptoms include illness, fatigue, vomiting, lack of appetite, a disorder in the elementary canal. Chronic hepatitis C. It is a long period infection and can be fatal if not treated properly. It causes serious health issues, such as damage to the liver, scarring of the liver, and even can cause cancer in the liver. Now, it is curable with oral tablets, by taking two to six months, daily. Cirrhosis also shows no symptoms until the whole liver is damaged. Some common symptoms are fatigue, loss of appetite, vomiting, inflammation in legs, and feet, loss of much weight, jaundice, loss of sexual activity in men, development of breasts, in women, improper periods, etc. HCV can also become the cause of liver cancer. Viruses change the combination of genes, which is called gene mutation in some cells of the liver. It causes the growth of abnormal cells in the liver due to cancer, liver cells are continuing to divide and can lead to death. HCV can be treated by using direct-acting antiviral (DAA) tablets. These tablets are very effective in curing the virus in about 92% of people. The patient should take these tablets for about ten to twelve weeks. These tablets include Baraclude, tenofovir, telbivudine. In 1989 Choo et al. detected HCV from the blood of a person and proved that it is not hepatitis A and hepatitis B. It was found that this new virus can affect 90% of the patient with non HAV and non-HBV in the US. Hepatitis C virus almost affected the entire world, about 24 hundred thousand people are only affected in the USA. It is estimated that in 2015 ten hundred thousand people died due to HCV. In 2016 most deaths are calculated in china, and japan due to HCV. Now, the more affected country in the world is Egypt, followed by Pakistan. In Pakistan, HCV affects all the provinces. It is estimated that patients of HCV in Punjab are 5.4%, Sindh 2.5%, KPK 6%, Baluchistan 25%, and Baltistan 3%. We can choose several

different precautions for controlling HCV such as taking blood or body fluid precautions, do not use a contaminated syringe, do not share your razor with anyone, safe your sexual activities, wear gloves during hospitalization. In 2019 Pitcher, A. B. et al. [1] presented an SCTZ model to prevent HVC via syringes. In 2009 Dahari, H. et al. [2] proposed a TIV model to study the propagation of HCV with high viral load. In 2005 Dahari, H. et al. discussed the TIVA model, to see the infection by HCV [3]. In 2019 Jia, W. et al [4] formulate a $SEI - aI_cTR$ model to control HCV in China. In 2007 Dahari, H. et al. [5] introduced the RTPE model to study the genomic sequence in HCV. In 2014 Mushayabasa, S. et al. presented a SIBA model to assess the impact of anti-viral medication [6]. In 2019 Lombardo, S. D. et al. [7] devised the TIVZWA model to check the impact of vaccination. In 2009 Reluga, T. C. et al. presented a TIV model to analyze the spread of sick and safe liver cells [8]. In 2019 Kalemera, M. et al. [9] designed a DEMM model to see entry criteria for HCV. In 2002 Ribeiro, R. M. et al. have presented an HIV model to analyze the behavior of nonlinear memory systems [10]. In 2016 Durfee, L. J. introduced the infection model to study HVC [11]. In 2015 Echevarria, D. et al. [12] studied the effect of the injected drug on viral load in Chicago. In 2013 Elbasha, E. H. presented epidemic Model for hepatitis C virus transmission [13]. In 2009 La Porte, F. et al. discussed the properties of HCV propagation during hemodialysis [14]. In 2019 Miller-Dickson, M. D et al. has designed the epidemic model to explain the HCV outbreak by injection drug [15]. In 2015 Cousin et al. proposed a new model to check the relationship between the infection, intensity, treatment, and negligence of HCV through injection drug [16]. In 2002 Avendan et al. [17] presented a new model to formulate the behavior of susceptible, infected, viral load and memory T cells for HCV. In 2019 Heffernan, A. et al. [18] suggested a standard for the eradication of HCV. In 2017 Hadi, H. A. proposed the TIV model to make the immune system strong against HCV [19]. In 2018 Aston, P. et al. [20] used the TIV model to demonstrate the efficacy of anti-viral medicine. For some more details about epidemic and physical models, see [21–25]. Fractional-order derivative is practical as compared to classical derivative because the dynamics of real phenomena can be broadly understood by fractional-order derivative due to its special features. The ordinary derivatives cannot choose the phenomenon at two distinct closed points. The generalization of the classical or integer-order calculus is fractional calculus. The first notion of the fractional-order derivative has been presented by L Hospital and Leibniz in 1695. The growing interest in the modeling of complex real-world issues with the use of fractional differential equations is due to its many features that cannot be obtained in the ordinary case. These characteristics permit fractional differential equations not only to model the non-markovian but also non-Gaussian phenomenon efficiently [26, 27]. To remove these drawbacks of the non-classical derivatives, different kinds of fractional derivatives were presented. Among them is the Atangana-Baleanu derivative, which is a nonlocal fractional derivative with the non-singular kernel, connected with many implementations [28].

Fractional calculus is one of the novelist types of calculus having a broad range of applications in many different scientific and engineering disciplines. The order of the derivatives in the fractional calculus might be any real number that separates the fractional calculus from the ordinary calculus where the derivatives are allowed only positive integers. Therefore, fractional calculus might be considered as an extension of ordinary calculus. Fractional calculus is a highly useful tool in the modeling of many sorts of scientific phenomena including image processing, earthquake engineering, biomedical engineering, and physics. Here, some fundamental concepts of fractional calculus [29, 30] and applications of it to different scientific and engineering areas are studied [31–37].

Even though fractional calculus is a highly useful and important topic, a general solution method that could be used at almost every sort of problem has not yet been established. Most of the solution techniques in this area have been developed for particular sorts of problems. As a result, a single standard method for problems regarding fractional calculus has not emerged. Therefore, finding reliable and accurate solution techniques along with fast implementation methods is very useful and is an active research area. Some well-known methods for the analytical and numerical solutions of fractional differential and integral equations might be listed as power series method, differential transform and, homotopy analysis method, variational iteration method, homotopy perturbation method, and Sinc–Galerkin method.

In this work, we have modified the classical hepatitis-C virus epidemic model into a fractal-fractional model by considering the fractal-fractional order operator. A novel numerical scheme is designed to find the numerical solutions and this novel scheme shows the steady-state solution of the underlying model. Furthermore, the new parameters pertinent to fractal and fractional order of the operator enhance the flexibility of the dynamics of the state variables which capture the real phenomenon more accurately. For instance, the immunity of individuals varies in different regions of the world depending upon the health conditions, environment, hygienic standards, food quality, pollution, and many others. So, the transmission rate for the disease dynamics cannot be the same in all the countries. It varies worldwide. The extended hepatitis-C virus epidemic model has the quality to fit better for many countries by adjusting the fractal and fractional order parameters. On the other hand, the classical model has no facility of this type.

This work has a more realistic approach. As the biological phenomenon contains memory effect and the classical epidemic models do not cover this important fact. This deficiency in the integer-order model enticed us to investigate the dynamics of the hepatitis-C virus in the fractal-fractional setup.

2. Preliminaries

In this section, we give some main definitions related to fractal-fractional derivatives and fractal-fractional integral.

Definition 2.1. Let the function $f(t)$ be continuous and fractal differentiable on some open interval say (a, b) with order ρ. Then, the fractal-fractional derivative of f in Riemann-Liouville sense with order σ having the generalized Mittag-Leffler type kernel is presented by [38]:

$$ {}^{FFM}_{c}D^{\sigma,\rho}_{t}u(t) = \frac{AB(\sigma)}{1-\sigma}\frac{d}{dt^{\rho}}\int_{a}^{t} f(z)E_{\sigma}\Big(\frac{-\sigma}{1-\sigma}(t-z)^{\sigma}\Big)dz,\ 0<\sigma,\rho\leq 1, \tag{2.1} $$

where, $AB(\sigma) = 1-\sigma+\frac{\sigma}{\Gamma(\sigma)}$.

Definition 2.2. The fractal-fractional integral of order σ of a function $f(t)$, continuous in some open interval say (a, b) corresponding to the fractal fractional derivative having Mittag-Leffler type kernel is given as [38]:

$$ {}^{FFM}_{0}I^{\sigma,\rho}_{t}u(t) = \frac{\sigma\rho}{AB(\sigma)}\int_{0}^{t} z^{\sigma-1}u(s)(t-z)^{\sigma-1}dz + \frac{\rho(1-\sigma)t^{\rho-1}}{AB(\sigma)}f(t). \tag{2.2} $$

Lemma 2.3. *We have the following relation between the fractal derivative and classical derivative.*

$$ \frac{df}{dt^{\sigma}} = \frac{1}{\sigma t^{\sigma-1}}f'(t). \tag{2.3} $$

3. Mathematical model and its stability

This section is devoted to the development of the extended fractal-fractional model and finding the local and global stability at equilibrium points.

We consider the following problem:

$$\begin{aligned}
\frac{dS}{dt} &= B - \left(kb_1a + kb_2c\right)S - \mu S \\
\frac{da}{dt} &= \left(kb_1a + kb_2c\right)S - (\sigma_1 + \mu)a \\
\frac{dc}{dt} &= \delta\sigma_1 a - (\sigma_2 + \mu)c \\
\frac{dr}{dt} &= (1-\delta)\sigma_1 a + \sigma c_2 - \mu r
\end{aligned}$$

Since the first-order derivatives capture the maximum rate of change, while the fractional-order derivatives contain the memory effect which is helpful in describing the phenomenon with a rate of dynamics, different from the maximum rate. Also, the rates of dynamics are not the same across the country or globe. That is why fractional differential operators are applied to overcome these types of problems.

A classical epidemic model of the hepatitis C virus is considered. Since the integer-order derivative is local by nature. So, they can measure the change in the neighborhood of a particular instant of time. But, the biological phenomenon is influenced by the events and measures that have been adopted in the past. Equivalently, they involve the memory effect. The fractional derivatives have the memory effect. Therefore, a biological phenomenon like a disease can be described more accurately. Moreover, the fractional-order differential operators improve the stability of the solution. These key facts motivated us to reshape the classical model.

$$\begin{aligned}
{}^{FFM}_{a}D_t^{\sigma,\rho}S(t) &= B - \left(kb_1a + kb_2c\right)S - \mu S && (3.1)\\
{}^{FFM}_{a}D_t^{\sigma,\rho}a(t) &= \left(kb_1a + kb_2c\right)S - (\sigma_1 + \mu)a && (3.2)\\
{}^{FFM}_{a}D_t^{\sigma,\rho}c(t) &= \delta\sigma_1 a - (\sigma_2 + \mu)c && (3.3)\\
{}^{FFM}_{a}D_t^{\sigma,\rho}r(t) &= (1-\delta)\sigma_1 a + \sigma c_2 - \mu r && (3.4)
\end{aligned}$$

The number of susceptible is denoted by $S(t)$, the number of acutely infected individuals is denoted by $a(t)$, the number of chronic carriers is denoted by $c(t)$ and the number of recovered is denoted by $r(t)$.

The parameters are described as B: represented as birth rate, the death rate (naturally) given as μ. When the susceptible hosts are infected, they transfer to the acute infection class with a force of infection λ, which depends on the rate of borrowing injecting equipment k, and the transmission rates (probabilities b_1,b_2) adopted. Where b_1 is the transmission probability per contact if the person was in its primary acute infection and b_2 is the transmission probability per contact if persons were a chronic carrier. An individual with primary acute infection moves out of that state with a rate σ_1, with a fraction

δ becoming chronic carriers and the remaining fraction, $(1-\delta)$ recovering completely. Chronic carrier individuals can still clear the virus with a rate σ_2, and move into the recovered state.

As $r(t)$ is not the part of first three equations of the system (3.1)–(3.4) therefore we can consider,

$$ {}_{a}^{FFM}D_{t}^{\sigma,\rho}S(t) = B - (kb_1a + kb_2c)S - \mu S \tag{3.5} $$

$$ {}_{a}^{FFM}D_{t}^{\sigma,\rho}a(t) = (kb_1a + kb_2c)S - (\sigma_1 + \mu)a \tag{3.6} $$

$$ {}_{a}^{FFM}D_{t}^{\sigma,\rho}c(t) = \delta\sigma_1 a - (\sigma_2 + \mu)c \tag{3.7} $$

First we discuss the equilibria of the model (3.5)–(3.7). For this, we put ${}_{a}^{FFM}D_{t}^{\sigma,\rho}S(t) = 0$, ${}_{a}^{FFM}D_{t}^{\sigma,\rho}a(t) = 0$, ${}_{a}^{FFM}D_{t}^{\sigma,\rho}c(t) = 0$. The disease free equilibrium (DFE) state is $D_1 = (S_1, a_1, c_1) = \left(\frac{\beta}{\mu}, 0, 0\right)$ and endemic equilibrium (EE) state is $E_1 = (S^*, a^*, c^*)$ where $S^* = \frac{(\sigma_1+\mu)(\sigma_2+\mu)}{kb_1(\sigma_2+\mu)+kb_2\delta\sigma_1}$, $a^* = \frac{B}{(\sigma+\mu)} - \frac{\mu(\sigma_2+\mu)}{kb_1(\sigma_2+\mu)+kb_2\delta\sigma_1}$ and $c^* = \frac{\delta\sigma_1 B}{(\sigma_1+\mu)(\sigma_2+\mu)} - \frac{\delta\sigma_1\mu}{kb_1(\sigma_2+\mu)+kb_2\delta\sigma_1}$. The reproductive value is $R_0 = \frac{B(kb_1(\sigma_2+\mu)+kb_2\delta\sigma_1)}{\mu(\sigma_1+\mu)(\sigma_2+\mu)}$. The Jacobian matrix for the system (3.5) and (3.6) is given as,

$$ J = \begin{bmatrix} -(kb_1a + kb_2c) - \mu & -kb_1S & -kb_2S \\ kb_1a + kb_2c & kb_1S - (\sigma_1 + \mu) & kb_2S \\ 0 & \delta\sigma_1 & -(\sigma_2 + \mu) \end{bmatrix} $$

Theorem 3.1. *The DFE, $D_1 = (S_1, a_1, c_1) = \left(\frac{\beta}{\mu}, 0, 0\right)$ is LAS if $R_o < 1$*

Proof. The Jacobean Matrix at D_1 is

$$ J(D_1) = \begin{bmatrix} -\mu & -\frac{kb_1B}{\mu} & -\frac{kb_2B}{\mu} \\ 0 & \frac{kb_1B}{\mu} - (\sigma_1 + \mu) & \frac{kb_2B}{\mu} \\ 0 & \delta\sigma_1 & -(\sigma_2 + \mu) \end{bmatrix} $$

$$ \lambda_1 = -\mu < 0 $$

$$ |J(D_1) - \lambda I| = \begin{vmatrix} \frac{kb_1B}{\mu} - (\sigma_1 + \mu) - \lambda & \frac{kb_2B}{\mu} \\ \delta\sigma_1 & -(\sigma_2 + \mu) - \lambda \end{vmatrix} = 0 $$

Put $\frac{kb_1B}{\mu} = u_1 > 0$,

$$ \frac{kb_2B}{\mu} = u_2 > 0 $$

$$ (\sigma_2 + \mu) = u_3 > 0 $$

$$ (\sigma_2 + \mu) = u_4 > 0 $$

$$ \begin{vmatrix} u_1 - u_3 - \lambda & u_2 \\ \delta\sigma_1 & -u_4 - \lambda \end{vmatrix} = 0 $$

$$ (u_1 - u_3 - \lambda)(-u_4 - \lambda) - u_2\delta\sigma_1 = 0 $$

$$ -u_1u_4 - u_1\lambda + u_3u_4 + u_3\lambda + \lambda u_4 + \lambda^2 - u_2\delta\sigma_1 = 0 $$

$$ \lambda^2 + \lambda(u_4 + u_3 - u_1) + (u_3u_4 - u_1u_4 - u_2\delta\sigma_1) = 0 $$

By using Routh-Hurwitz Criterion of 2^{nd} order,

$$u_4 + u_3 - u_1 > 0$$

$$\Rightarrow (\sigma_2 + \mu) + (\sigma_1 + \mu) - \frac{kb_1 B}{\mu} > 0$$

$$\Rightarrow (\sigma_2 + \sigma_1 + 2\mu) > \frac{kb_1 B}{\mu}$$

$$\Rightarrow \frac{kb_1 B}{\mu(\sigma_2 + \sigma_1 + 2\mu)} < 1$$

$$\Rightarrow R_o < 1$$

and $u_3u_4 - u_1u_4 - u_2\delta\sigma_1 > 0$ $u_3u_4 > u_1u_4 + u_2\delta\sigma_1$ If $R_o < 1$ □

Theorem 3.2. *The EE, $E_1 = (S^*, a^*, c^*)$ is LAS If $R_o > 1$.*

Proof. The Jacobean Matrix at E_1 is

$$J(E_1) = \begin{bmatrix} -(kb_1a^* + kb_2c^*)S^* - \mu & -kb_1S^* & -kb_2S^* \\ kb_1a^* + kb_2c^* & kb_1S^* - (\sigma_1 + \mu) & kb_2S^* \\ 0 & \delta\sigma_1 & -(\sigma_2 + \mu) \end{bmatrix}$$

$$\begin{aligned} &|J(E_1) - \lambda| \\ &= \begin{vmatrix} -(kb_1a^* + kb_2c^*)S^* - \mu - \lambda & -kb_1S^* & -kb_2S^* \\ kb_1a^* + kb_2c^* & kb_1S^* - (\sigma_1 + \mu) - \lambda & kb_2S^* \\ 0 & \delta\sigma_1 & -(\sigma_2 + \mu) - \lambda \end{vmatrix} = 0 \\ &-\delta\sigma_1 \begin{vmatrix} -(kb_1a^* + kb_2c^*)S^* - \mu - \lambda & -kb_2S^* \\ kb_1a^* + kb_2c^* & kb_2S^* \end{vmatrix} \\ &-[(\sigma_2 + \mu) + \lambda] \begin{vmatrix} -(kb_1a^* + kb_2c^*)S^* - \mu - \lambda & -kb_1S^* \\ kb_1a^* + kb_2c^* & kb_1S^* - (\sigma_1 + \mu) - \lambda \end{vmatrix} = 0 \\ &-\delta\sigma_1 \begin{vmatrix} -A_1 - \mu - \lambda & -A_2 \\ A_1 & A_2 \end{vmatrix} - [A_4 + \lambda] \begin{vmatrix} -A_1 - \mu - \lambda & -A_3 \\ A_1 & A_3 - A_5 - \lambda \end{vmatrix} = 0 \end{aligned}$$

Where $A_1 = kb_1a^* + kb_2c^*$

$$A_2 = kb_2S^*$$

$$A_3 = kb_1S^*$$

$$A_4 = (\sigma_2 + \mu)$$

$$A_5 = (\sigma_1 + \mu)$$

$$\begin{aligned} &\lambda^3 + \lambda^2(A_1 + \mu + A_4 + A_5 - A_3) + \lambda[A_4(A_1 + \mu) \\ &+ (A_1 + \mu)(A_3 - A_5) + A_1A_3 - A_2\delta\sigma_1 + A_4(A_5 - A_3)] \\ &+ [(A_5 - A_3)(A_1 + \mu)A_4 + A_1A_3A_4 - \delta\sigma_1A_2\mu] = 0 \end{aligned}$$

By using Routh–Hurwitz Criterion of 3rd order

$$A_1 + A_4 + A_5 + \mu - A_3 > 0,$$
$$(A_5 - A_3)(A_1 + \mu)A_4 + A_1A_3A_4 - \delta\sigma_1A_2\mu > 0,$$
$$(A_1 + A_4 + A_5 + \mu - A_3)\left[(A_4 + A_3 - A_5)(A_1 + \mu) + A_1A_3 - \delta\sigma_1A_2 + A_4(A_5 - A_3)\right]$$
$$> \left[(A_5 - A_3)(A_1 + \mu)A_4 + A_1A_3A_4 - \delta\sigma_1A_2\mu\right]$$

□

Theorem 3.3. *For system (3.5)–(3.7) the disease free for equilibrium D_1 is G.A.S if $R_0 < 1$*

Proof. Let us define a Volterra Lyapunov function as

$$u = \left(S - S_1 - S_1 ln\frac{S}{S_1}\right) + a + c$$

Now by using lemma 1 and lemma 2 given in [39]

$$\begin{aligned}
{}_a^{FFM}D_t^{\sigma,\rho}u(t) &= \left(1 - \frac{S}{S_1}\right) \ {}_a^{FFM}D_t^{\sigma,\rho}S(t) + {}_a^{FFM}D_t^{\sigma,\rho}a(t) + {}_a^{FFM}D_t^{\sigma,\rho}c(t) \\
&= \left(1 - \frac{S}{S_1}\right)(B - (kb_1a + kb_2c)S - \mu S) + (kb_1a + kb_2c)S - (\sigma_1 + \mu)a + \sigma_1a - (\sigma_1 + mu)c \\
&= -\frac{(S - S_1)^2B}{SS_1} - kb_1(a - a_1)(S - S_1) - kb_2(S - S_1)(c - c_1) - a\mu(1 - \frac{kb_1S}{\mu}) \\
&- c\mu(1 - \frac{kb_2S}{\mu}) - \sigma_2c
\end{aligned}$$

So, ${}_a^{FFM}D_t^{\sigma,\rho}u(t) < 0$ for $R_0 < 1$ and ${}_a^{FFM}D_t^{\sigma,\rho}u(t) = 0$ if $S = S_1$, $a = 0$ and $c = 0$. Thus D_1 is G.A.S.

□

4. Main results

There are some other numerical techniques in the literature such as Adam Bashforth and methods constructed by using Newton's polynomial method [40, 41]. These schemes also show some good features. In this manuscript, our proposed scheme shows a reliable solution as it gives a steady-state solution. Also, our proposed scheme is simple and user-friendly as it involves less number of steps. There are many uncovered features of the proposed scheme to be explored.

We consider the following problem:

$$\frac{dS}{dt} = B - (kb_1a + kb_2c)S - \mu S$$
$$\frac{da}{dt} = (kb_1a + kb_2c)S - (\sigma_1 + \mu)a$$
$$\frac{dc}{dt} = \delta\sigma_1a - (\sigma_2 + \mu)c$$

We replace the classical derivatives with the fractal-fractional derivatives and we obtain:

$$
\begin{aligned}
{}^{FFM}_{a}D_{t}^{\sigma,\rho}S(t) &= B-(kb_1a+kb_2c)S-\mu S\\
{}^{FFM}_{a}D_{t}^{\sigma,\rho}a(t) &= (kb_1a+kb_2c)S-(\sigma_1+\mu)a\\
{}^{FFM}_{a}D_{t}^{\sigma,\rho}c(t) &= \delta\sigma_1 a-(\sigma_2+\mu)c
\end{aligned}
$$

For simplicity, we define

$$
\begin{aligned}
A(t,S,a,c) &= \rho t^{\rho-1}\left(B-(kb_1a+kb_2c)S-\mu S\right)\\
B(t,S,a,c) &= \rho t^{\rho-1}\left((kb_1a+kb_2c)S-(\sigma_1+\mu)a\right)\\
C(t,S,a,c) &= \rho t^{\rho-1}\left(\delta\sigma_1 a-(\sigma_2+\mu)c\right)
\end{aligned}
$$

Then, we get

$$
\begin{aligned}
\frac{AB(\sigma)}{1-\sigma}\frac{d}{dt}\int_0^t S(\tau)E_\alpha\left(\frac{-\sigma}{1-\sigma}(t-\tau)^\sigma\right)d\tau &= A(t,S,a,c)\\
\frac{AB(\sigma)}{1-\sigma}\frac{d}{dt}\int_0^t I(\tau)E_\alpha\left(\frac{-\sigma}{1-\sigma}(t-\tau)^\sigma\right)d\tau &= B(t,S,a,c)\\
\frac{AB(\sigma)}{1-\sigma}\frac{d}{dt}\int_0^t R(\tau)E_\alpha\left(\frac{-\sigma}{1-\sigma}(t-\tau)^\sigma\right)d\tau &= C(t,S,a,c)
\end{aligned}
$$

Applying the AB integral yields

$$
\begin{aligned}
S(t)-S(0) &= \frac{1-\sigma}{AB(\sigma)}A(t,S,a,c)+\frac{\sigma}{AB(\sigma)\Gamma(\sigma)}\int_0^t(t-\tau)^{\sigma-1}A(\tau,S,a,c)d\tau\\
a(t)-a(0) &= \frac{1-\sigma}{AB(\sigma)}B(t,S,a,c)+\frac{\sigma}{AB(\sigma)\Gamma(\sigma)}\int_0^t(t-\tau)^{\sigma-1}B(\tau,S,a,c)d\tau\\
c(t)-c(0) &= \frac{1-\sigma}{AB(\sigma)}C(t,S,a,c)+\frac{\sigma}{AB(\sigma)\Gamma(\sigma)}\int_0^t(t-\tau)^{\sigma-1}C(\tau,S,a,c)d\tau
\end{aligned}
$$

We discretize these equations at t_{n+1} as:

$$
\begin{aligned}
S^{n+1} &= S^0+\frac{1-\sigma}{AB(\sigma)}A(t_{n+1},S^n,a^n,c^n)\\
&\quad+\frac{\sigma}{AB(\sigma)\Gamma(\sigma)}\int_0^{t_{n+1}}(t_{n+1}-\tau)^{\sigma-1}A(\tau,S,a,c)d\tau\\
a^{n+1} &= a^0+\frac{1-\sigma}{AB(\sigma)}B(t_{n+1},S^n,a^n,c^n)\\
&\quad+\frac{\sigma}{AB(\sigma)\Gamma(\sigma)}\int_0^{t_{n+1}}(t_{n+1}-\tau)^{\sigma-1}B(\tau,S,a,c)d\tau\\
c^{n+1} &= c^0+\frac{1-\alpha}{AB(\sigma)}C(t_{n+1},S^n,a^n,c^n)\\
&\quad+\frac{\sigma}{AB(\sigma)\Gamma(\sigma)}\int_0^{t_{n+1}}(t-\tau)^{\sigma-1}C(\tau,S,a,c)d\tau
\end{aligned}
$$

Then, we obtain

$$
\begin{aligned}
S^{n+1} &= S^0 + \frac{1-\sigma}{AB(\sigma)} A(t_{n+1}, S^n, a^n, c^n) \\
&\quad + \frac{\sigma}{AB(\sigma)} \sum_{p=0}^{n} \left[\frac{h^\sigma A(t_p, S^n, a^n, c^n)}{\Gamma(\sigma+2)} \left((n+1-p)^\sigma (n-p+2+\sigma) \right.\right. \\
&\quad \left.\left. -(n-p)^\sigma (n-p+2+2\sigma) \right) \right] \\
&\quad - \frac{\sigma}{AB(\sigma)} \sum_{p=0}^{n} \left[\frac{h^\sigma A(t_{p-1}, S^{n-1}, a^{n-1}, c^{n-1})}{\Gamma(\sigma+2)} \left((n+1-p)^{\sigma+1} \right.\right. \\
&\quad \left.\left. -(n-p)^\sigma (n-p+1+\sigma) \right) \right] \\
a^{n+1} &= a^0 + \frac{1-\sigma}{AB(\sigma)} B(t_{n+1}, S^n, a^n, c^n) \\
&+ \frac{\sigma}{AB(\sigma)} \sum_{p=0}^{n} \left[\frac{h^\sigma B(t_p, S^n, a^n, c^n)}{\Gamma(\sigma+2)} \left((n+1-p)^\sigma (n-p+2+\sigma) \right.\right. \\
&\quad \left.\left. -(n-p)^\sigma (n-p+2+2\sigma) \right) \right] \\
&\quad - \frac{\sigma}{AB(\sigma)} \sum_{p=0}^{n} \left[\frac{h^\sigma B(t_{p-1}, S^{n-1}, a^{n-1}, c^{n-1})}{\Gamma(\sigma+2)} \left((n+1-p)^{\sigma+1} \right.\right. \\
&\quad \left.\left. -(n-p)^\sigma (n-p+1+\sigma) \right) \right] \\
c^{n+1} &= c^0 + \frac{1-\sigma}{AB(\sigma)} C(t_{n+1}, S^n, a^n, c^n) \\
&+ \frac{\sigma}{AB(\sigma)} \sum_{p=0}^{n} \left[\frac{h^\sigma C(t_p, S^n, a^n, c^n)}{\Gamma(\sigma+2)} \left((n+1-p)^\sigma (n-p+2+\sigma) \right.\right. \\
&\quad \left.\left. -(n-p)^\sigma (n-p+2+2\sigma) \right) \right] \\
&\quad - \frac{\sigma}{AB(\sigma)} \sum_{p=0}^{n} \left[\frac{h^\sigma C(t_{p-1}, S^{n-1}, a^{n-1}, c^{n-1})}{\Gamma(\sigma+2)} \left((n+1-p)^{\sigma+1} \right.\right. \\
&\quad \left.\left. -(n-p)^\sigma (n-p+1+\sigma) \right) \right]
\end{aligned}
$$

by the method using in [42].

The fractal and fractional epidemic model for the hepatitis-C virus model is solved to obtain the numerical solutions. The proposed method addresses the fractal parameters as well as the fractional order parameter. Considering both the parameters of the epidemic model, the picture of disease dynamics has become more comprehensive and clearer. So, the role of fractal and fractional parameters are studied analytically and graphically. Therefore, with the help of this proposed method, more epidemic models can be studied in a better way. Also, this is help in future prediction of the disease. The proposed method is formulated to solve the fractal fractional model of infection disease model. This method converges towards the true steady state of the model. Also, this technique can easily be applied to obtain the steady state solutions namely, the virus free state and endemic state. When the value of the fractal order parameter are changed, a new trajectory of the state variables obtained, which

converges towards the exact fixed point with a different rate of convergence. This fact has a significant role to capture the dynamics of a particular real world scenario.

The existing schemes are more complicated for the application point of view. The proposed method is a value addition in the existing literature. The reliability of the scheme may be studied in future, when more models will be solved by applying this design. Furthermore, when exact solution is not available for the comparison, steady states become more important to study the efficacy of the scheme. The proposed scheme successfully, attains the exact steady state of the model.

5. Numerical simulations

In this segment, simulated graphs are illustrated against the different values of parameters, fractional order and fractal dimensions. These graphs show some important features of the state variables. The values of parameters involved in the system (3.5)–(3.7) for DFE state are, $B = 0.5$, $b_1 = 0.003, 0.003$, $\sigma_1 = 0.1$, $\sigma_2 = 0.01$ and $\delta = 0.80$. Similarly the parametric values of the system (3.5)–(3.7) for EE state are, $B = 0.5$, $b_1 = 0.1$, $b_2 = 0.1$, $\sigma_1 = 0.1$, $\sigma_2 = 0.01$ and $\delta = 0.80$. The initial conditions of the system (3.5)–(3.7) are $S(0) = 0.4$, $a(0) = 0.2$ and $c(0) = 0.1$

Figure 1 illustrates the growth of the susceptible state variable $S(t)$ with respect to time t, graphically at a disease-free state. The fractional-order ρ is kept fixed as 0.95 for this situation and the fractal parameter σ is changed to investigate its role in the progression of the susceptible persons. The different curved graphical lines show the effect of change in the value of $\sigma$when the value of ρ is kept fixed for all the cases. Each graph attains the exact DFE, by following a different route for converging towards the mathematically evaluated value. The simulated graphs that, for a greater value of σ the rate of convergence is high as compared to the smaller value of σ. Also, the different tracks of the graphs ultimately coincide with the true equilibrium point. The parametric value is chosen systematically which makes the R_0 less than one.

Likewise, Figure 2 demonstrate the progression of the acutely infected individuals of hepatitis-c virus. The graph advance towards the DFE against the different value of σ. The value of $A(t)$ becomes zero in the interval $(0, T)$ when $T > 0$ and $t \in (0, T)$.

The value of σ does not affect the value of DFE. It simply adjusts the rate of convergence. In this case, also, the value of the parameters is the same as were in Figure 1. Moreover, the value of $R_0 < 1$. The sketches in Figure 3 show the graphical behavior of the chronic carriers with respect to time. The graphs describe that value of $C(t)$ decreases gradually and ultimately it becomes zero after a due course of time. Other conditions on parameters are the same for instance, the value of $R_0 < 1$ and the value of control parameters and kept fixed. Figure 4 shows the graphical behavior of $S(t)$ at endemic equilibrium state. The number of susceptible persons in the graph decreases at a certain level, then it heads towards the disease existing steady-state and hits at the true value of the steady-state. The different graphical templates are drowned against the different values of fractal parameter σ, these templates reflect that each trajectory, plotted against a different value of σ, converges towards the true steady state. But, the rate of convergence of each trajectory is different, depending upon the value of fractal order σ.

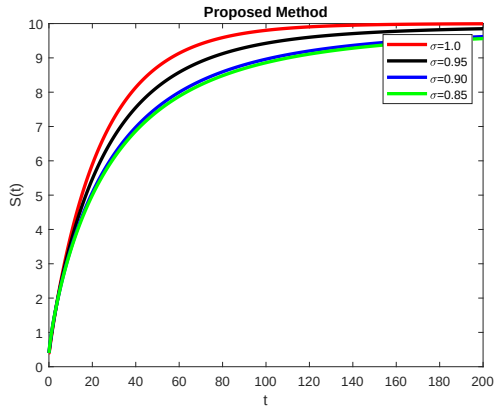

Figure 1. Graphical behavior of $S(t)$ with various values of fractional order σ with $\rho = 0.95$ at DFE point.

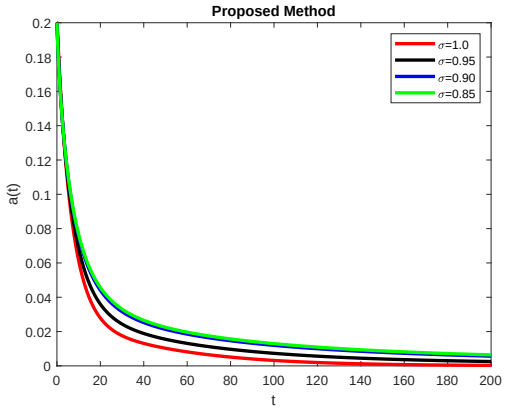

Figure 2. Graphical behavior of $a(t)$ with various values of fractional order σ with $\rho = 0.95$ at DFE point.

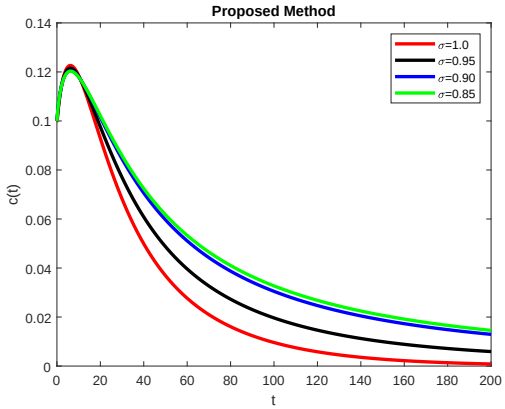

Figure 3. Graphical behavior of $c(t)$ with various values of fractional order σ with $\rho = 0.95$ at DFE point.

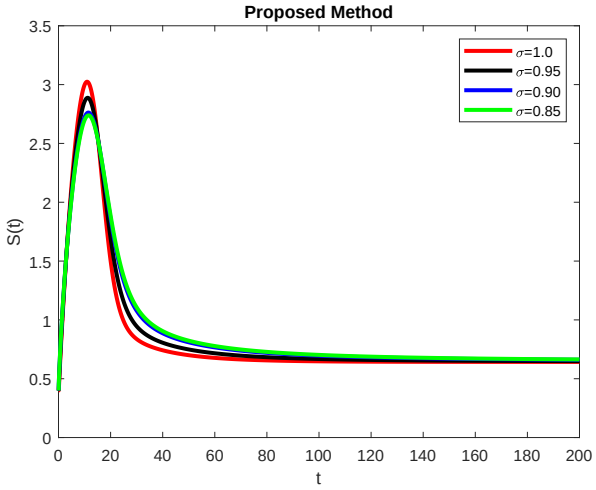

Figure 4. Graphical behavior of $S(t)$ with various values of fractional order σ with $\rho = 0.95$ at EE point.

Figure 5 reflects the course of dynamics for the acutely affected populace at the disease's existing steady-state. The graphs in the figure show that initially, the size of $A(t)$ increases because the disease is spreading in the population at this stage. Then after a certain time period, the graphs heads towards the fixed state and coincide with the analytical value. Each graph attains the required state with a specific rate. This rate depends entirely on the value of the fractal parameter when other parametric values are kept fixed. The behavior of the chronic carriers $C(t)$ is represented by the graph in Figure 6. The graph sketched in this figure is drowned for suitable selected parametric values that make the basic reproductive number $R_0 > 1$. The value of $C(t)$ grows with the passage of time. Then after attaining some specific value, The curve turns towards the desired steady state. Also, every graph attains the fixed state, at different times, which shows the different rates of convergence.

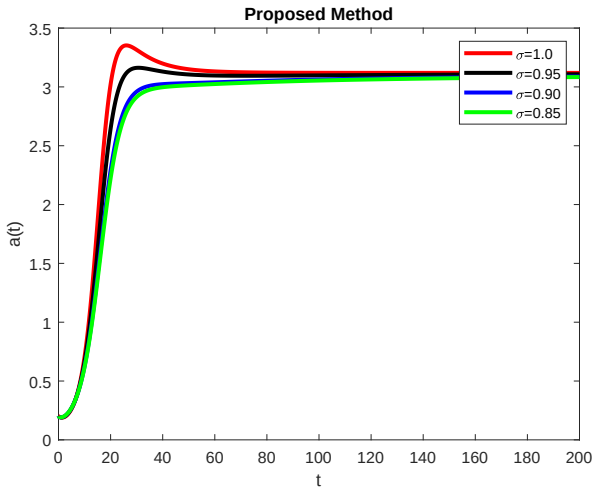

Figure 5. Graphical behavior of $a(t)$ with various values of fractional order σ with $\rho = 0.95$ at EE point.

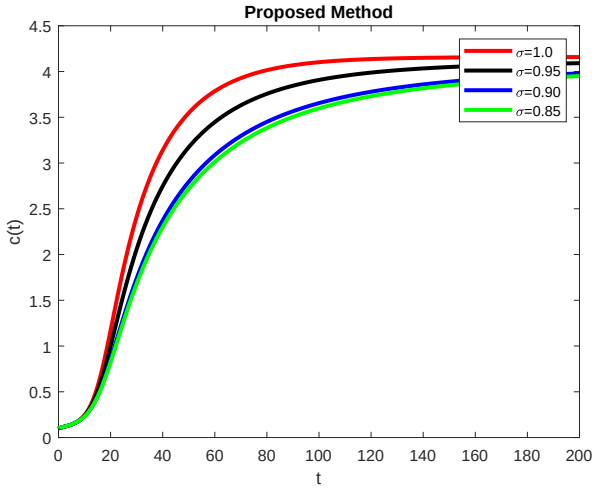

Figure 6. Graphical behavior of $c(t)$ with various values of fractional order σ with ρ = 0.95 at EE point.

The numerical graphs in Figures 7–9 reveal the behavior of the state variables involved in the epidemic system. The main target, of these simulations, is to authenticate the role of fractional order, ρ, which is now considered as 0.93. The values of all other parameters are kept unchanged, while the values of fractal dimension are highlighted in each figure. This time the curved templates also, meet the disease-free state. The only difference that is observed from the graphs, is the alteration in the rate of convergence. Now, the rate is smaller as compared to the graphs with ρ = 0.95. So, it can be said that the rate of convergence and order of fractional derivatives are attached with a direct relation. Now, the time to reach the DFE state is comparatively large. Therefore, the value of ρ, the order of the fractional differential operator controls the rate of convergence. Similarly, the numerical designs in Figures 10–12 reflect the behavior of the disease progression in various compartments of the model. All the curved designs in every figure advance towards the right position and direction. In these graphs, the values of ρ are taken as 0.93. Other parametric values are considered as these were in Figures 1–6.

Every graph in Figures 10–12 meets the exact steady-state i.e., EE state. Here, the curved trajectories take more time to attain the endemic equilibrium position. It is mentionable that ρ, the fractional-order parameter restricts the disease dynamics before attaining the desired state. Hence, all the graphs in Figures 1–12 show that the presented method is a reliable tool to solve the infectious disease phenomenon. It has been investigated that when the values of fractional order parameter are closer to one, the memory effect lasts for a short interval of time and is called short memory, and, when the value of the fraction order parameter approaches zero, the memory effect lasts for a long time and it is called long-term memory. Do the numerical graphs reflect that the graph with short memory converges fastly, towards the true steady-state i.e., for σ is closer to one. Moreover, when the value of σ is decreased, the rate of convergence towards the true equilibrium point decrease. In the nutshell, when the short memory is considered, the rate of convergence is fast as compared to the rate of convergence, when the memory effect lasts for a long time.

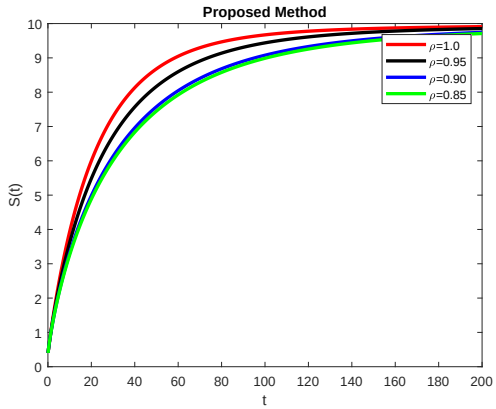

Figure 7. Graphical behavior of $S(t)$ with various values of fractal order ρ with σ = 0.93 at DFE point.

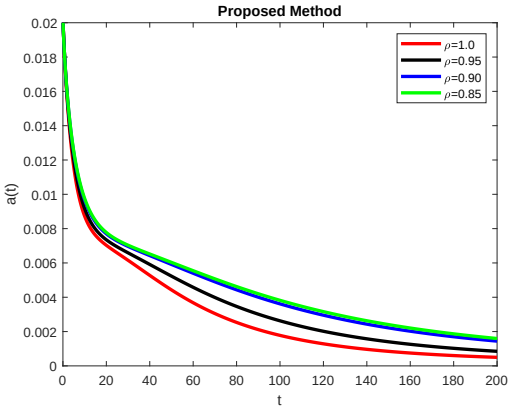

Figure 8. Graphical behavior of $a(t)$ with various values of fractal order ρ with σ = 0.93 at DFE point.

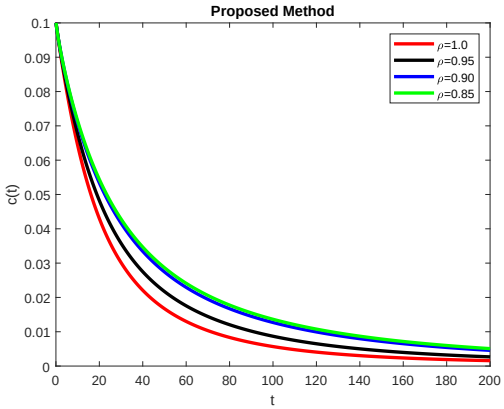

Figure 9. Graphical behavior of $c(t)$ with various values of fractal order ρ with σ = 0.93 at DFE point.

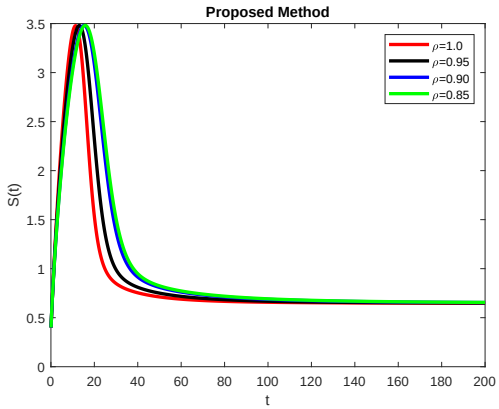

Figure 10. Graphical behavior of $S(t)$ with various values of fractal order ρ with σ = 0.93 at EE point.

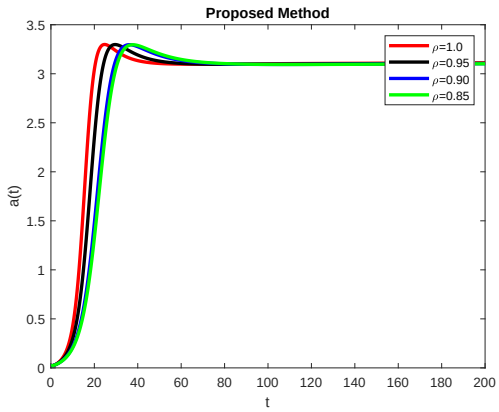

Figure 11. Graphical behavior of $a(t)$ with various values of fractal order ρ with σ = 0.93 at EE point.

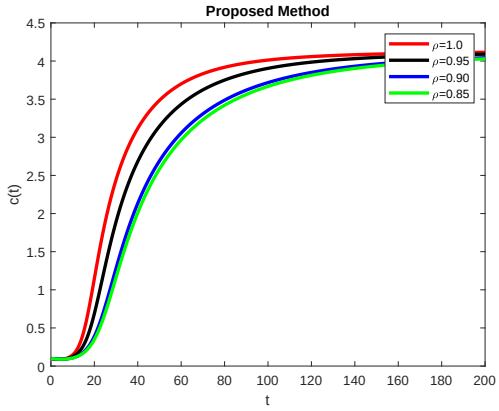

Figure 12. Graphical behavior of $c(t)$ with various values of fractal order ρ with σ = 0.93 at EE point.

6. Conclusions

In this study, a hepatitis C virus epidemic model is successfully studied. Two types of stable states, disease-free and endemic steady state are described. Moreover, the local stability for both of the steady-state is examined. It is observed that a disease-free stable state is locally asymptotically stable if $R_0 < 1$ and the same behavior is obtained for endemic state for $R_0 > 1$. The Routh-Hurwitz procedure is followed to determine the stability of the system. Similarly, the global stability of the model is ascertained at DFE. Before, all the above-mentioned facts, the classical model is remodeled to obtain a fractal-fractional hepatitis C infection model. Numerical simulations are presented to verify the progression of the state variables at both of the steady states.

Acknowledgements

The authors would like to thank the reviewers for their valuable comments.

Conflict of interest

The authors declare no conflict of interest.

References

1. A. B. Pitcher, A. Borquez, B. Skaathun, N. K. Martin, Mathematical modeling of hepatitis c virus (HCV) prevention among people who inject drugs, *J. Theor. Biol.*, **481** (2019), 194–201. http://dx.doi.org/10.1016/j.jtbi.2018.11.013
2. H. Dahari, J. E. Layden-Almer, E. Kallwitz, R. M. Ribeiro, S. J. Cotler, T. J. Layden, et al., A mathematical model of hepatitis C virus dynamics in patients with high baseline viral loads or advanced liver disease, *Gastroenterology*, **136** (2009), 1402–1409. http://dx.doi.org/10.1053/j.gastro.2008.12.060
3. H. Dahari, M. Major, X. Zhang, K. Mihalik, C. M. Rice, A. S. Perelson, et al., Mathematical modeling of primary hepatitis C infection: non-cytolytic clearance and early blockage of virus production, *Gastroenterology*, **128** (2005), 1056–1066. http://dx.doi.org/10.1053/j.gastro.2005.01.049
4. W. Jia, J. Weng, C. Fang, Y. Li, A dynamic model and some strategies on how to prevent and control hepatitis c in mainland China, *BMC Infect. Dis.*, **19** (2019), 724. http://dx.doi.org/10.1186/s12879-019-4311-x
5. H. Dahari, R. M. Ribeiro, C. M. Rice, A. S. Perelson, Mathematical modeling of sub genomic hepatitis C virus replication in Huh-7 cells, *J. Virol.*, **81** (2007), 750–760. http://dx.doi.org/10.1128/JVI.01304-06
6. S. Mushayabasa, C. P. Bhunu, Mathematical analysis of hepatitis C model for intravenous drug misusers: impact of antiviral therapy, abstinence and relapse, *Simulation*, **90** (2014), 487–500. http://dx.doi.org/10.1177/0037549714528388

7. S. D. Lombardo, S. Lombardo, Global stability for a mathematical model of hepatitis C: Impact of a possible vaccination with DAAs therapy, *AIP Conference Proceedings*, **2159** (2019), 030020. http://dx.doi.org/10.1063/1.5127485

8. T. C. Reluga, H. Dahari, A. S. Perelson, Analysis of hepatitis C virus infection models with hepatocyte homeostasis, *SIAM J. Appl. Math.*, **69** (2009), 999–1023. http://dx.doi.org/10.1137/080714579

9. M. Kalemera, D. Mincheva, J. Grove, G. J. Illingworth, Building a mechanistic mathematical model of hepatitis C virus entry, *PLoS Comput. Biol.*, **15** (2019), e1006905. http://dx.doi.org/10.1371/journal.pcbi.1006905

10. R. M. Ribeiro, A. Lo, A. S. Perelson, Dynamics of hepatitis B virus infection. *Microbes Infect.*, **4** (2002), 829–835. http://dx.doi.org/10.1016/s1286-4579(02)01603-9

11. L. J. Durfee, Bio-mathematics: Introduction to the mathematical model of the hepatitis C virus, *Electronic Theses, Projects, and Dissertations*, 2016, 428.

12. D. Echevarria, A. Gutfraind, B. Boodram, M. Major, S. Del Valle, S. J. Cotler, et al., Mathematical modeling of hepatitis C prevalence reduction with antiviral treatment scale-up in persons who inject drugs in metropolitan Chicago, *PLoS ONE*, **10** (2015), e0135901. http://dx.doi.org/10.1371/journal.pone.0135901

13. E. H. Elbasha, Model for hepatitis C virus transmissions, *Math. Biosci. Eng.*, **10** (2014), 1045–1065. http://dx.doi.org/10.3934/mbe.2013.10.1045

14. F. Laporte, G. Tap, A. Jaafar, K. Saune-Sandres, N. Kamar, L. Rostaing, et al., Mathematical modeling of hepatitis C virus transmission in hemodialysis, *Americal Journal of Infection Control*, **37** (2009), 403–407. http://dx.doi.org/10.1016/j.ajic.2008.05.013

15. M. D. Miller-Dickson, V. A. Meszaros, S. Almagro-Moreno, O. C. Brandon, Hepatitis C virus modelled as an indirectly transmitted infection highlights the centrality of injection drug equipment in disease dynamics, *J. R. Soc. Interface*, **16** (2019), 20190334. http://dx.doi.org/10.1098/rsif.2019.0334

16. A. Cousien, V. C. Tran, S. Deuffic-Burban, M. Jauffret-Roustide, J. S. Dhersin, Y. Yazdanpanah, Dynamic modelling of hepatitis C virus transmission among people who inject drugs: a methodological review, *J. Viral Hepatitis*, **22** (2015), 213–229. http://dx.doi.org/10.1111/jvh.12337

17. R. Avendano, L. Esteva, J. A. Flores, J. F. Allen, G. Gomez, J. Lopez-Estrada, A mathematical model for the dynamics of hepatitis C, *Comput. Math. Method. Med.*, **4** (2002), 461260. http://dx.doi.org/10.1080/10273660290003777

18. A. Heffernan, G. S. Cooke, S. Nayagam, M. Thursz, T. B. Hallett, Scaling up prevention and treatment towards the elimination of hepatitis C, *The Lancet*, **393** (2019), 1319–1329. http://dx.doi.org/10.1016/S0140-6736(18)32277-3

19. H. A. Hadi, A mathematical model of hepatitis C virus infection incorporating immune responses and cell proliferation, M.S. Thesis of The University of Texas, 2017.

20. P. Aston, K. Cranfield, H. O'Farrell, A. Cassenote, C. J. Mendes-Correa, A. Segurado, et al., Hepatitis C viral dynamics using a combination therapy of interferon, ribavirin, and telaprevir: mathematical modeling and model validation, In: *Hepatitis C–From infection to cure*, IntechOpen, 2018. http://dx.doi.org/10.5772/intechopen.75761

21. A. Raza, A. Ahmadian, M. Rafiq, S. Salahshour, M. Ferrara, An analysis of a nonlinear susceptible-exposed-infected-quarantine-recovered pandemic model of a novel coronavirus with delay effect, *Results Phys.*, **21** (2021), 103771. http://dx.doi.org/10.1016/j.rinp.2020.103771

22. N. Ghorui, A. Ghosh, S. P. Mondal, M. Y. Bajuri, A. Ahmadian, S. Salahshour, et al., Identification of dominant risk factor involved in spread of COVID-19 using hesitant fuzzy MCDM methodology, *Results Phys.*, **21** (2021), 103811. http://dx.doi.org/10.1016/j.rinp.2020.103811

23. M. Zamir, K. Shah, F. Nadeem, M. Y. Bajuri, A. Ahmadian, S. Salahshour, et al., Threshold conditions for global stability of disease free state of COVID-19, *Results Phys.*, **21** (2021), 103784. http://dx.doi.org/10.1016/j.rinp.2020.103784

24. S. Ahmad, A. Ullah, K. Shah, S. Salahshour, A. Ahmadian, T. Ciano, Fuzzy fractional-order model of the novel coronavirus, *Adv. Differ. Equ.*, **2020** (2020), 472. http://dx.doi.org/10.1186/s13662-020-02934-0

25. A. Ahmadian, N. Senu, F. Larki, S. Salahshour, M. Suleiman, M. S. Islam, A legendre approximation for solving a fuzzy fractional drug transduction model into the bloodstream, In: *Recent advances on soft computing and data mining*, Cham: Springer, 2014, 25–34. http://dx.doi.org/10.1007/978-3-319-07692-8_3

26. H. M. Srivastava, V. P. Dubey, R. Kumar, J. Singh, D. Kumar, D. Baleanu, An efficient computational approach for a fractional-order biological population model with carrying capacity, *Chaos Soliton. Fract.*, **31** (2020), 109880. http://dx.doi.org/10.1016/j.chaos.2020.109880

27. J. Singh, Analysis of fractional blood alcohol model with composite fractional derivative, *Chaos Soliton. Fract.*, **140** (2020), 110127. http://dx.doi.org/10.1016/j.chaos.2020.110127

28. E. Bonyah, R. Zarin, Fatmawati, Mathematical modeling of Cancer and Hepatitis co-dynamics with non-local and non-singular kernel, *Commun. Math. Biol. Neurosci.*, **2020** (2020), 91. http://dx.doi.org/10.28919/cmbn/5029

29. R. E. Gutierrez, J. M. Rosario, J. T. Machado, Fractional order calculus: basic concepts and engineering applications, *Math. Probl. Eng.*, **2010** (2010), 375858. http://dx.doi.org/10.1155/2010/375858

30. J. T. Machado, Fractional calculus: fundamentals and applications, In: *Acoustics and vibration of mechanical structures–VMS-2017*, Cham: Springer, 2018, 3–11. http://dx.doi.org/10.1007/978-3-319-69823-6_1

31. T. A. Biala, A. Q. M. Khaliq, A fractional-order compartmental model for the spread of the COVID-19 pandemic, *Commun. Nonlinear Sci. Numer. Simulat.*, **98** (2021), 105764. http://dx.doi.org/10.1016/j.cnsns.2021.105764

32. Z. Iqbal, N. Ahmed, D. Baleanu, W. Adel, M. Rafiq, M. Aziz-ur Rehman, et al., Positivity and boundedness preserving numerical algorithm for the solution of fractional nonlinear epidemic model of HIV/AIDS transmission, *Chaos. Soliton. Fract.*, **134** (2020), 109706. http://dx.doi.org/10.1016/j.chaos.2020.109706

33. Z. Iqbal, N. Ahmed, D. Baleanu, M. Rafiq, M. S. Iqbal, M. Aziz-ur Rehman, Structure preserving computational technique for fractional order Schnakenberg model, *Comp. Appl. Math.*, **39** (2020), 61. http://dx.doi.org/10.1007/s40314-020-1068-1

34. M. Alqhtani, K. M. Saad, Numerical solutions of space-fractional diffusion equations via the exponential decay kernel, *AIMS Mathematics*, **7** (2022), 6535–6549. http://dx.doi.org/10.3934/math.2022364

35. M. Alqhtani, K. M. Saad, Fractal-fractional Michaelis-Menten enzymatic reaction model via different kernels, *Fractal Fract.*, **6** (2022), 13. http://dx.doi.org/10.3390/fractalfract6010013

36. K. M. Saad, J. F. Gomez-Aguilar, A. A. Almadiy, A fractional numerical study on a chronic hepatitis C virus infection model with immune response, *Chaos Soliton. Fract.*, **139** (2020), 110062. http://dx.doi.org/10.1016/j.chaos.2020.110062

37. K. M. Saad, M. Alqhtani, Numerical simulation of the fractal-fractional reaction diffusion equations with general nonlinear, *AIMS Mathematics*, **6** (2021), 3788–3804. http://dx.doi.org/10.3934/math.2021225

38. A. Atangana, Fractal-fractional differentiation and integration: Connecting fractal calculus and fractional calculus to predict complex system, *Chaos Soliton. Fract.*, **102** (2017), 396–406. http://dx.doi.org/10.1016/j.chaos.2017.04.027

39. N. Sene, SIR epidemic model with Mittag-Leffler fractional derivative, *Chaos Soliton. Fract.*, **137** (2020), 109833. http://dx.doi.org/10.1016/j.chaos.2020.109833

40. P. Liu, M. Rahman, A. Din, Fractal fractional based transmission dynamics of COVID-19 epidemic model, *Computer Methods in Biomechanics and Biomedical Engineering*, 2022, in press. http://dx.doi.org/10.1080/10255842.2022.2040489

41. J. Zhou, S. Salahshour, A. Ahmadian, N. Senu, Modeling the dynamics of COVID-19 using fractal-fractional operator with a case study, *Results Phys.*, **33** (2022), 105103. http://dx.doi.org/10.1016/j.rinp.2021.105103

42. M. Toufik, A. Atangana, New numerical approximation of fractional derivative with non-local and non-singular kernel: application to chaotic models, *Eur. Phys. J. Plus*, **132** (2017), 444. http://dx.doi.org/10.1140/epjp/i2017-11717-0

AIMS Press